

## White emitting CdS quantum dot nanoluminophores hybridized on near-ultraviolet LEDs for high-quality white light generation and tuning

Sedat Nizamoglu<sup>1,2</sup>, Evren Mutlugun<sup>1,3</sup>, Ozgun Akyuz<sup>1</sup>,  
Nihan Kosku Perkgoz<sup>1</sup>, Hilmi Volkan Demir<sup>1,2,3,5</sup>,  
Lydia Liebscher<sup>4</sup>, Sameer Sapra<sup>4</sup>, Nikolai Gaponik<sup>4</sup>  
and Alexander Eychmüller<sup>4</sup>

<sup>1</sup> Nanotechnology Research Center, Bilkent University, Ankara 06800, Turkey

<sup>2</sup> Department of Electrical and Electronics Engineering, Bilkent University, Ankara 06800, Turkey

<sup>3</sup> Department of Physics, Bilkent University, Ankara 06800, Turkey

<sup>4</sup> Physikalische Chemie, TU Dresden, Bergstr. 66b, 01062 Dresden, Germany

E-mail: [volkan@bilkent.edu.tr](mailto:volkan@bilkent.edu.tr) and [sameer.sapra@chemie.tu-dresden.de](mailto:sameer.sapra@chemie.tu-dresden.de)

*New Journal of Physics* **10** (2008) 023026 (9pp)

Received 28 December 2007

Published 18 February 2008

Online at <http://www.njp.org/>

doi:10.1088/1367-2630/10/2/023026

**Abstract.** To generate white light using semiconductor nanocrystal (NC) quantum dots integrated on light emitting diodes (LEDs), multiple hybrid device parameters (emission wavelengths of the NCs and the excitation platform, order of the NCs with different sizes, amount of the different types of NCs, etc) need to be carefully designed and properly implemented. In this study, we introduce and demonstrate white LEDs based on simple device hybridization using only a single type of white emitting CdS quantum dot nanoluminophores on near-ultraviolet LEDs. Here we present their design, synthesis-growth, fabrication and characterization. With these hybrid devices, we achieve high color rendering index (>70), despite using only a single NC type. Furthermore, we conveniently tune their photometric properties including the chromaticity coordinates, correlated color temperature, and color rendering index with the number of hybridized nanoluminophores in a controlled manner.

<sup>5</sup> Author to whom any correspondence should be addressed.

Semiconductor nanocrystal (NC) quantum dots feature important optical properties essential for their use as luminophores in light emitting devices, including size-dependent tunability of emission, large photoluminescence (PL) quantum yield, and high photostability [1]. Additionally, the ability to deposit their thin films easily and uniformly with common techniques such as spin casting and dip coating makes them also attractive for use in layered device architectures [2]. Consequently, NCs are considered to hold great promise for future solid state applications. To this end significant progress has been achieved in NC based device applications in recent years [3]–[18].

Lighting is one of the next solid state frontiers. Recently important scientific achievements have been made using NC emitters at this frontier. In the previous work of our group, white light generation using CdSe/ZnS core-shell NCs in multiple combinations emitting in different spectral ranges, hybridized with blue InGaN/GaN light emitting diodes (LEDs), has been successfully demonstrated [11]–[13]. Also, a blue/green dual-wavelength InGaN/GaN LED integrated with a single type of red emitting CdSe NCs has been previously shown to generate white light [14]. Additionally, in our previous work, white light generation with high-color rendering index using dual hybridization of both fluorescent polymers and luminescent NCs on LEDs has been reported [15]. Furthermore, white LEDs (WLEDs) have also been realized by integrating a blended mixture of CdSeS NCs in polymethylmethacrylate (PMMA) on ultraviolet LEDs (UV LEDs) [16] and using layer-by-layer assembly of CdSe/ZnS NCs on near-UV (n-UV) LEDs [17, 18].

As the state of the art, such white light generation based on the use of NC luminophores relies on the collective PL contributed from the combination of different types of NC emitters or on the luminescence arising from the combination of both NCs and LEDs. However, in all of these approaches to obtain white light, the hybrid WLED device parameters including the type and concentration of NCs and the thickness and order of the NC films are required to be carefully designed and properly implemented at the device level.

As a conceptual advance in this study, we introduce and demonstrate WLEDs with simple device hybridization using only white emitting CdS quantum dot nanoluminophores on our n-UV LEDs, to achieve high color rendering index despite using a single NC type. In this work, for the first time, solely by controlling the number of the nanoluminophores hybridized on the LEDs, we conveniently tune and set the photometric properties of the resulting hybrid LEDs including the chromaticity coordinates, correlated color temperature, and color rendering index. Figure 1 shows the tristimulus chromaticity coordinates of a set of such hybrid WLEDs, tuned in a very controlled manner with the amount of their hybridized white emitting CdS nanoluminophores, on the CIE 1931 chromaticity diagram. In our previous work, when only one type of NC (e.g., yellow) is used on a blue LED, white light generation has been possible only with a color rendering index of 15 [11]. But here by using only a single type of CdS NCs, we achieve color rendering indices higher than 70. Therefore, the use of such white emitting nanoluminophores for hybrid device application provides important benefits of simpler device engineering while providing higher color rendering index.

In this paper, we present the design, synthesis-growth, fabrication, and characterization of white emitting CdS nanoluminophore hybridized WLEDs. To study their photometric properties, we use the three main photometric figures of merit [19]: the tristimulus coordinates, the correlated color temperature, and the color rendering index. Firstly,  $(x, y)$  tristimulus chromaticity coordinates show the location of the light source on the CIE chromaticity diagram to define the perceived color of its emission spectrum. Secondly, the color temperature ( $T_c$ )

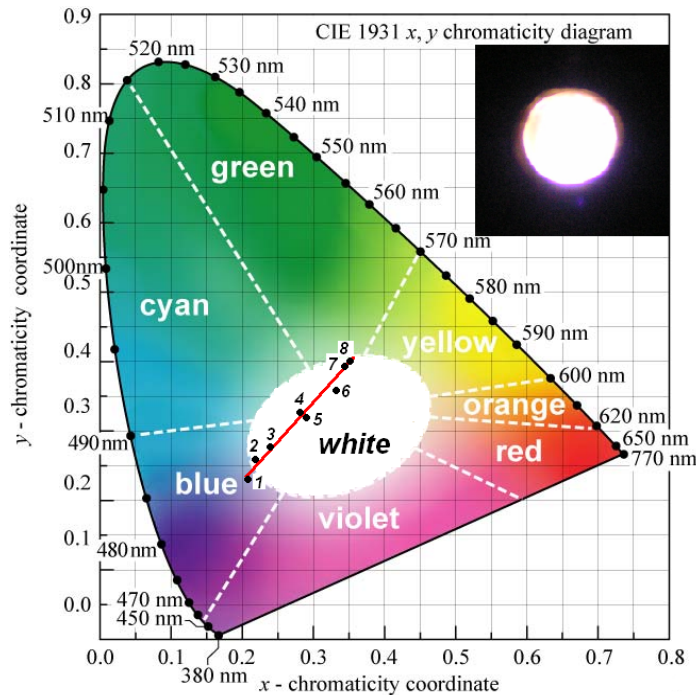


**Figure 1.**  $(x, y)$  tristimulus chromaticity coordinates of white emitting CdS nanoluminophores tuned with their amount hybridized on the LEDs across the white region on the chromaticity diagram.

reveals the warmness–coolness perception of the generated white light, ranging from warm-white to cool-white, by indicating the position of the light source on the planckian locus in the chromaticity diagram, if it is a blackbody radiator. If not, instead, the correlated color temperature is used to indicate the corresponding color temperature of the blackbody radiator that is closest in color to the light source in the untransformed chromaticity coordinates, i.e., in  $(u', v')$ . Thirdly, the color rendering index ( $R_a$ ) shows the extent to which the light source reflects the true color of physical objects it illuminates, in a scale of  $-100$  to  $100$ .

For white light generation we synthesized trap-rich CdS NC luminophores. The synthesis of CdS NCs was carried out at a Schlenk line under argon atmosphere.  $0.1$  mmol CdO was dissolved in  $4$  ml octadecene using  $0.6$  mmol oleic acid at  $\sim 200$  °C. The temperature was then raised to  $250$  °C. A  $0.1$  M sulfur solution was prepared separately by dissolving elemental S in octadecene.  $0.5$  ml of the S solution was injected into the hot Cd solution at  $250$  °C and heated for  $5$  min. The solution was immediately cooled down and the NCs precipitated and redissolved in toluene. Our CdS surface state emitting (SSE) NCs with a typical dot diameter of  $2$ – $3$  nm were found to exhibit a relatively higher quantum efficiency of  $17\%$ , as also studied and reported in the previous work of Sapra *et al* [20]. As an alternative to these CdS NCs, magic-sized CdSe NCs with a diameter of  $1$ – $2$  nm are known to generate white light, but their quantum efficiency is found to be restricted to only  $2$ – $3\%$ . Thus such CdS NCs are more attractive for use as luminophores. When optically pumped, the surface states of these CdS NC luminophores give rise to a broad emission band that spans the entirety of the visible spectrum. As a result of pumping with a light source at higher photon energy than their effective band gap energy, the

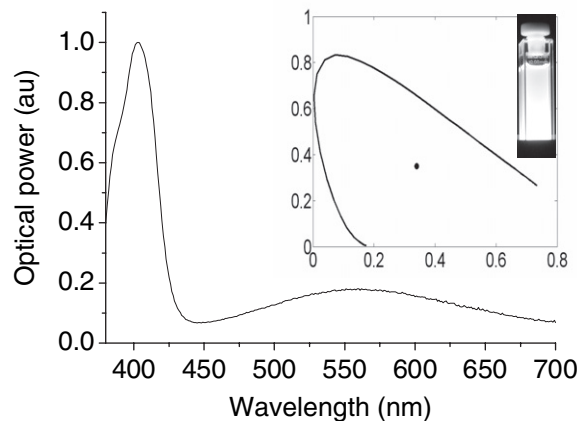


**Figure 2.** The PL spectrum of CdS SSE NCs in toluene solution. The corresponding  $(x, y)$  chromaticity coordinates and a photograph of the white light generated by these CdS NCs in toluene under UV excitation are also provided in the inset.

radiative recombination through the interband and mid-gap states takes place and, consequently, white light is generated. In this work the particle diameter of our CdS luminophores was about 2.4 nm, as inferred from the absorption edge at 400 nm [21, 22]. The narrow peaks of their absorption spectrum (with a half width at half maximum (HWHM) of 14 nm) and their emission spectrum (with a full width at half maximum (FWHM) of 22 nm) indicate a very narrow size distribution of these NCs. Figure 2 presents the PL spectrum of these synthesized CdS NCs. This PL spectrum corresponds to chromaticity coordinates of  $(x = 0.34, y = 0.35)$ , a correlated color temperature of 5146 K, and a color rendering index of 82.5, when in toluene solution.

To generate white light at the chip scale, we fabricated n-UV emitting InGaN/GaN based LEDs as the high-energy photon source. The growth of these InGaN/GaN LEDs was carried out using a metal organic chemical vapor deposition (MOCVD) system (Aixtron RF200/4 RF-S). On a *c*-plane sapphire, first a 14 nm thick GaN nucleation layer and then a 200 nm thick GaN buffer layer were grown. This buffer layer was particularly important to increase the crystal quality. Subsequently, a 690 nm thick Si-doped n-type GaN epitaxial layer and five 2–3 nm thick InGaN wells and GaN barriers were grown at a growth temperature of 720 °C. Finally, a 4-nm thick Mg-doped p-type GaN layer, a 50 nm thick Mg-doped p-type AlGaN layer, and a 120 nm thick Mg-doped GaN layer were grown as the contact layers. The epitaxial growth was monitored by *in situ* optical reflectance, and the growth temperature was controlled using two infrared pyrometers. After finishing the growth, Mg dopants were activated at 750 °C for 15 min. Further for the definition of device mesas and electrical contacts, the standard semiconductor processing procedures followed photolithography, thermal evaporation (metallization), reactive ion etch (RIE), and rapid thermal annealing, as also carried out in our previous work [23]–[26]. To lay down n-contacts, the epitaxial wafer was etched with RIE down to reach the n-contact layer and a 10 nm thick Ti film with a 200 nm over-layer of Al was deposited. The metallization was completed with a subsequent rapid thermal annealing at 600 °C for 1 min under nitrogen to prevent the oxidization. For the p-contacts, the metal deposition of a 15 nm thick Ni film was followed with a 100 nm over-layer of Au, which was further cured with rapid thermal annealing at 700 °C for 30 s.

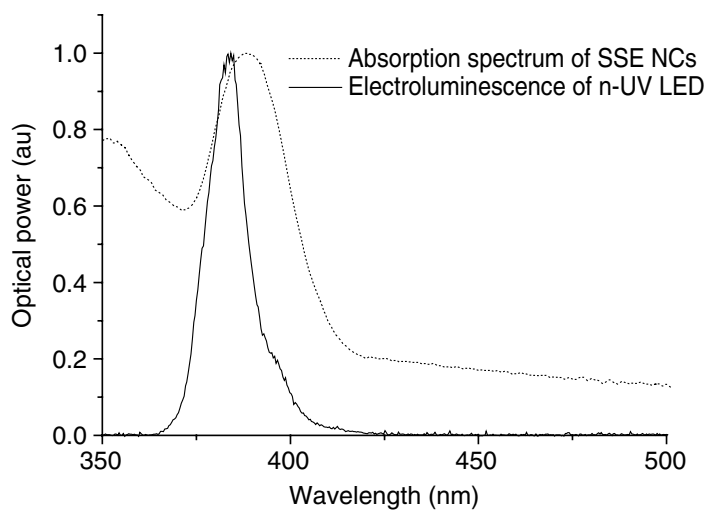


**Figure 3.** The electroluminescence spectrum of the n-UV InGaN/GaN LED along with the matching absorption spectrum of the white emitting CdS NC luminophores.

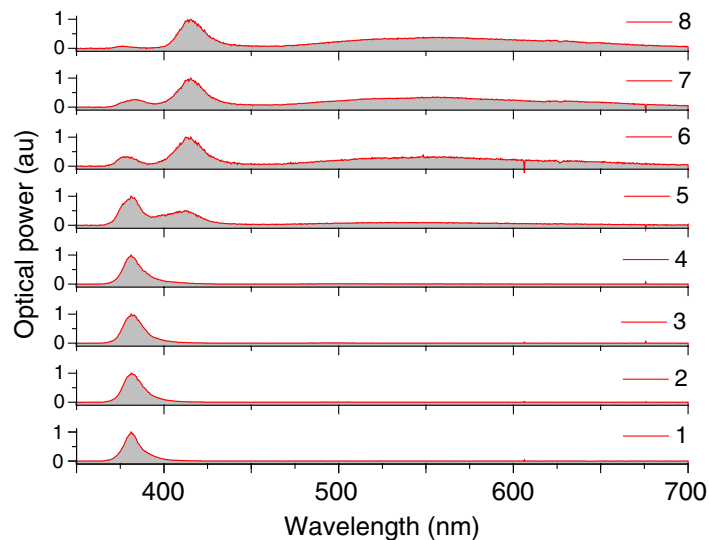
The white emitting CdS nanoluminophores that are photoexcited by the n-UV InGaN/GaN LED generate white light at the nanoscale and contribute to the white light generation at the chip scale. In this work, all of the hybrid devices were implemented using InGaN/GaN LED pump sources with a peak wavelength of 383 nm in the n-UV. Here, the use of an n-UV LED offers several advantages. Firstly, the electroluminescence peak of the n-UV LED at 383 nm overlaps with the excitonic absorption peak of the SSE NCs as shown in figure 3, thus making the resulting optical pumping efficient. Secondly, another important advantage is that n-UV LEDs with high output optical powers (e.g., up to 5 W) are required for other high-technology applications and their production in the short term has been already announced (e.g., by Nichia [27]). Therefore, for future lighting applications, it is critical to develop and demonstrate hybrid light sources on UV pumping platforms.

For the hybridization of CdS NCs on the n-UV InGaN/GaN LED (with a die area of 7 mm  $\times$  7 mm), 1 ml NC solution with a concentration of 11.3 nmol ml<sup>-1</sup> was used. First, approximately ten times more acetone was added and the solution was centrifuged to precipitate the NCs. Afterwards, 500  $\mu$ l PMMA solution was added to the precipitated NCs and the NCs were then dispersed in PMMA host in an ultrasonic bath. By heating the NC-PMMA and the chip substrate at 70 °C on a hot plate to have a better NC film quality, the NCs were hybridized in the PMMA matrix with drop casting on the backside of an LED chip. After each hybridized droplet with a volume of 20  $\mu$ l, 10–15 min were allowed for solidification of the NC film during post-baking. The resulting hybrid LEDs were characterized on a probe station with dc probes placed on the LEDs to electrically drive them in forward bias by a current power supply (HP4142B Modular dc Source/Monitor). The emitted light was then collected by a multimode fiber positioned normal to the surface of the die and the fiber was connected to an optical spectrum analyzer setup (Ocean Optics PC2000 with an optical resolution of 0.5 nm).

In these hybrid devices, our main parameter to tune their photometric properties is the number of NCs hybridized on the LEDs. The NC amount affects the level of conversion from incident photons to emitted/transmitted photons for the NC layer as explained in detail

**Table 1.** The photometric properties of the hybrid white nanoluminophore-LEDs (samples 1–8).

Sample	$x$	$y$	$T_c$ (K)	$R_a$
1	0.21	0.23	34463	57.3
2	0.22	0.26	30159	62.1
3	0.24	0.28	16174	66.3
4	0.28	0.33	8259	72.6
5	0.29	0.32	7586	73.2
6	0.33	0.36	5564	73.4
7	0.34	0.39	5154	74.6
8	0.35	0.40	4718	74.9

**Figure 4.** The emission spectrum of WLEDs (samples 1–8) hybridized with white emitting CdS NCs in PMMA film (in integer multiples of 45.2 nmol) when electrically driven.

below. Therefore, the ability to control the NC number makes it possible to tune the resulting white light spectrum. Figure 4 presents the optical emission spectra of the implemented hybrid WLEDs (samples 1–8). In figure 4, while the emission peaking at 383 nm corresponds to the electroluminescence of n-UV LED, the emission at 400–425 nm corresponds to the interband transition of the NC luminophores, and the remaining broad emission across 450–700 nm corresponds to their surface state emission. As the number of hybridized NCs is increased (from sample 1 to sample 8), the relative intensity of the electroluminescence coming from the n-UV LED at 383 nm becomes weaker and the PL coming from the NCs becomes stronger. The modified emission spectrum in turn tunes the optical properties including the  $(x, y)$  chromaticity coordinates, correlated color temperature ( $T_c$ ), and color rendering index ( $R_a$ ). These are summarized in table 1 for samples 1–8, prepared with the hybridization of CdS SSE NC in integer multiples of 45.2 nmol.

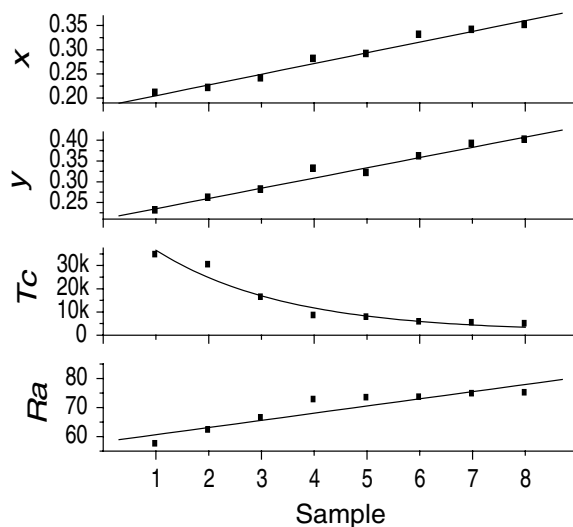


**Figure 5.**  $x$ - and  $y$ -coordinates, color temperature and color rendering index of hybrid WLEDs.

When the number of hybridized NCs increases, the  $(x, y)$  chromaticity coordinates increase and the correlated color temperature decreases, as shown in figure 5. We consider different tuning mechanisms to be responsible for the effect of varying the number of hybridized NCs. Firstly, as the NC number is increased, the reabsorption probability of the generated photons is increased, too. Because of the existing size distribution of the NCs with a 22 nm FWHM as observed in solution emission, the probability of reabsorption is observed to increase proportionally with the number of NCs due to the fact that one photon coming from a NC can encounter many more states having lower band gap energies. We thus observe the influence of reabsorption by examining the relative luminescence ratio of the trap states emission (in the interval of 450–700 nm) to the interband emission (with a peak wavelength around 410 nm) as shown in figure 6. When the NCs are cast into solid film with a relatively high concentration of  $2.3 \mu\text{mol ml}^{-1}$  corresponding to an interdot spacing of approximately 10 nm, the trap states absorb more of the generated photons by interband transitions and lower energy trap states and the emission of trap states becomes stronger with respect to the in-solution luminescence having low concentration ( $<1 \text{ nmol ml}^{-1}$ ). Secondly, as the number of NCs is increased, the contribution coming from the n-UV LED in the chromaticity diagram is decreased. As shown in figure 1, the violet part is in the lower left of the white region on the CIE chromaticity diagram and the electroluminescence of the n-UV LED corresponds to the tristimulus coordinates of (0.1731, 0.0049) near the blue region. Thirdly, another effective mechanism of the red shift is the effect of changing the dielectric environment from solution (toluene) to the solid film (PMMA) and effectively increasing with increasing NC density. For the interband transition in the case of in-solution CdS NCs, the PL peak wavelength is detected at 403.0 nm. However, when these NCs are embedded into a solid PMMA film, for example, in the case of sample 8 as shown in figure 6, the PL peak wavelength shifts to 414.7 nm. Here, the asymmetric narrowing of interband luminescence comes from the reabsorption of NCs. Because of these mechanisms, with increasing the number of NCs from sample 1 to sample 8, the tristimulus coordinates are tuned from the blue region to the red region on the chromaticity diagram. This makes

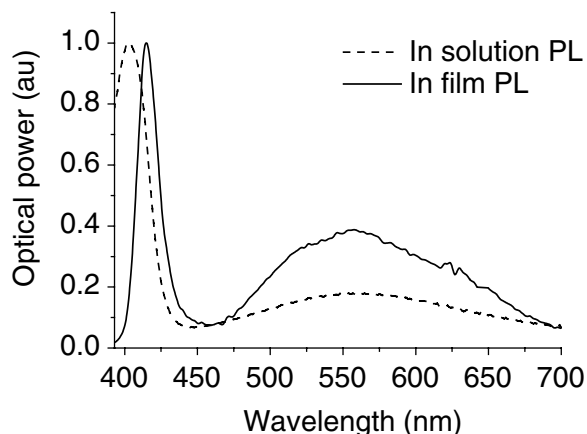


**Figure 6.** PL of CdS nanoluminophores in solution and in film (sample 8).

the resulting white light warmer, decreasing the color temperature, and the resulting emission spectrum better spread across the visible, increasing the color rendering index.

Examining the photometric properties of these hybrid WLEDs, sample 1 exhibits a color rendering index of 57.3 that is near to white in the blue region on the CIE chromaticity diagram in figure 1. As the thickness of the hybridized NC films is increased, the corresponding tristimulus coordinates shift into the white region and the color rendering index increases. In our previous work, we demonstrated a color rendering index of 71.0 by the hybridization of four different types of NCs on a blue LED [10]. In this work, we obtain a higher color rendering index of 74.9 using only a single type of NC. Using CdS SSE NCs is thus advantageous in different aspects. First, assembling different types of NCs layer by layer on top of each other is a harder, lower-yield process than hybridization of only single type of NCs as in this work. Additionally, when making the hybridization of various sizes of NCs with different band gaps, the absorption of NC emission by other NCs with narrower band gaps needs to be also taken into account. For example, if red-emitting NCs are placed on top of the cyan NCs on the LED, the red NCs absorb the emitted photons in cyan. In the case of using multiple combination of NCs, this makes the implementation rather complicated. On the contrary, in this approach of using single NCs in this work, the device engineering becomes much easier, while obtaining better performance.

In conclusion, we synthesized white emitting CdS nanoluminophores with quantum efficiency of 17% for hybrid device applications, which show benefits in terms of simpler device engineering while providing good device performance. We demonstrated high-quality white light generation with the hybridization of these white CdS nanoluminophores on InGaN/GaN n-UV LEDs with high color rendering indices  $>70$ . Furthermore, we tuned their white light parameters with the amount of the NCs hybridized on LEDs. Our proof-of-concept demonstrations in this work indicated that using a single type of such CdS NC luminophores is more advantageous than using multiple combinations of NCs and that these hybrid white nanoluminophore-LEDs are promising candidates for future solid-state lighting applications.



## Acknowledgments

This work is supported by EU-PHOREMOST Network of Excellence 511616. Other support includes Marie Curie European Reintegration Grant MOON 021391 and TUBITAK under the project no EEEAG 106E020, 104E114, 107E088, 107E297, 105E065 and 105E066. HVD also acknowledges additional support from the Turkish National Academy of Sciences Distinguished Young Scientist Award (TUBA GEBIP) and the European Science Foundation European Young Investigator Award (ESF EURYI).

## References

- [1] Achermann M, Petruska M A, Kos S, Smith D L, Koleske D D and Klimov V I 2004 *Nature* **429** 642
- [2] Heliotis G, Gu E, Griffin C, Jeon C W, Stavrinou P N, Dawson M D and Bradley D D C 2006 *J. Opt. A: Pure Appl. Opt.* **8** 445
- [3] Somers R, Bawendi M G and Nocera D G 2007 *Green Chem.* **9** 403
- [4] Somers R C, Bawendi M G and Nocera D G 2007 *Chem. Soc. Rev.* **36** 579
- [5] Anikeeva P O, Halpert J E, Bawendi M G and Bulovic V 2007 *Nano Lett.* **8** 2196
- [6] Gur I, Fromer N A, Geier M L and Alivisatos A P 2005 *Science* **310** 462
- [7] Huynh W U, Dittmer J J and Alivisatos A P 2002 *Science* **295** 2425
- [8] Soganci I M, Nizamoglu S, Mutlugun E, Akin O and Demir H V 2007 *Opt. Express* **15** 14289
- [9] Bertoni C, Gallardo D, Dunn S, Gaponik N and Eychmüller A 2007 *Appl. Phys. Lett.* **90** 034107
- [10] Mutlugun E, Soganci I M and Demir H V 2007 *Opt. Express* **15** 1128
- [11] Nizamoglu S, Ozel T, Sari E and Demir H V 2007 *Nanotechnology* **18** 065709
- [12] Nizamoglu S, Ozel T, Sari E and Demir H V 2006 *IEEE COMMAD WO-A5*
- [13] Chen H, Hsu C and Hong H 2006 *IEEE Photonics Technol. Lett.* **18** 193
- [14] Chen H, Yeh D, Lu C, Huang C, Shiao W, Huang J, Yang C C, Liu I and Su W 2006 *IEEE Photonics Technol. Lett.* **18** 1430
- [15] Demir H V, Nizamoglu S, Ozel T, Mutlugun E, Huyal I O, Sari E, Holder E and Tian N 2007 *New J. Phys.* **9** 362
- [16] Ali M, Chattopadhyay S, Nag A, Kumar A, Sapra S, Chakraborty S and Sarma D D 2007 *Nanotechnology* **18** 075401
- [17] Nizamoglu S and Demir H V 2007 *J. Opt. A: Pure Appl. Opt.* **9** S419
- [18] Nizamoglu S and Demir H V 2007 *Nanotechnology* **18** 405702
- [19] Schubert E F 2006 *Light-Emitting Diodes* (Cambridge: Cambridge University Press)
- [20] Sapra S, Mayilo S, Klar T A, Rogach A L and Feldmann J 2007 *Adv. Mater.* **19** 569
- [21] Viswanatha R, Sapra S, Saha-Dasgupta T and Sarma D D 2005 *Phys. Rev. B* **72** 045333
- [22] Sapra S and Sarma D D 2004 *Phys. Rev. B* **69** 125304
- [23] Sari E, Nizamoglu S, Ozel T and Demir H V 2007 *Appl. Phys. Lett.* **90** 011101
- [24] Sabnis V A, Demir H V, Fidaner O, Harris J S, Miller D A B, Zheng J F, Li N, Wu T C, Chen H T and Houg Y M 2004 *Appl. Phys. Lett.* **84** 469
- [25] Demir H V, Sabnis V A, Zheng J F, Fidaner O, Harris J S and Miller D A B 2004 *IEEE Photonics Technol. Lett.* **16** 2305
- [26] Ozel T, Sari E, Nizamoglu S and Demir H V 2007 *J. Appl. Phys.* **102** 113101
- [27] Sandhu A 2007 *Nat. Photonics* **1** 38